Supporting Information for Generalizable Mechanochemical Impact of Curvature Governing Stability and Reactivity at Catalytic Sites on Rippled Supports

Sayan Banerjee* and Sampad Mandal

Department of Chemistry, University of Tennessee–Knoxville, Knoxville, TN 37923, USA

Table of Contents

1. Computational Details and Benchmarking

All density functional theory (DFT) calculations were performed using the Quantum Espresso software package.[1] The generalized gradient approximation (GGA) with the Perdew–Burke–Ernzerhof (PBE) exchange–correlation functional was employed.[2] Ultrasoft GBRV pseudopotentials were used with kinetic-energy and charge-density cutoffs of 35 Ry and 350 Ry, respectively.[3] Dispersion interactions were included via the DFT-D3 correction developed by Grimme and co-workers.[4] A (6×6) graphene supercell was used to investigate the effect of curvature on adsorption, with a vacuum spacing of approximately 20 Å along the surface normal to eliminate spurious periodic interactions. A Γ-centered ($2 \times 2 \times 1$) Monkhorst–Pack grid was used to sample the Brillouin zone.[5]

To ensure consistent rumpling amplitude and sinusoidal curvature profiles, a single hydrogen atom was placed near the crest (convex) region in all simulations. The hydrogen atom was positioned away from the M–N_4 center, as shown in Figure S2, for the four curvature values studied. The purpose of this placement is to preserve the curvature pattern across geometries, enabling energetic quantification at the convex sites, which are otherwise unstable compared to concave regions. In the absence of this auxiliary H atom, the surface undergoes significant structural relaxation, leading to inconsistent curvature magnitudes. An alternative strategy would be to fix selected atoms to maintain curvature, but this would restrict the relaxation to local minima. Including an H atom allows the structure to reach the minima while maintaining the desired curvature profile.

The presence of this additional H atom does not introduce artificial effects on the local geometry or electronic structure.[6] While it may cause minor quantitative shifts in adsorption energies, it does not alter the qualitative curvature trends. This was confirmed by formation energy calculations performed both with and without the additional H atom, which yielded identical metal-dependent trends (Figure S1).

Adsorption (binding) energies of H and CO_2 were computed as

$$\Delta E_{\mathrm{H}} = E_{\mathrm{H}^*} - E_{\mathrm{bare}} - E_{\mathrm{H}}, \tag{1}$$

$$\Delta E_{\mathrm{CO_2}} = E_{\mathrm{CO_2^*}} - E_{\mathrm{bare}} - E_{\mathrm{CO_2}}, \tag{2}$$

where E_{H^*} and $E_{\mathrm{CO_2^*}}$ correspond to the total energies of the adsorbed systems, and E_{bare}, E_{H}, and $E_{\mathrm{CO_2}}$ denote the total energies of the clean slab, gas-phase H atom, and isolated CO_2 molecule, respectively. Formation energies (E_f) were calculated as

$$E_f = E_{\mathrm{slab+M}} - E_{\mathrm{slab}} - E_{\mathrm{M}}. \tag{3}$$

The bonding s-band center, $\varepsilon_s^{\mathrm{bond}}$, is defined as

$$\varepsilon_s^{\mathrm{bond}} = \frac{\displaystyle\int_{E_{\mathrm{min}}}^{E_F} E\, D_s(E)\, dE}{\displaystyle\int_{E_{\mathrm{min}}}^{E_F} D_s(E)\, dE}, \tag{4}$$

where $D_s(E)$ is the s-projected density of states (PDOS), and E_{min} denotes the lower integration limit, chosen sufficiently below the valence manifold (typically $E_{\mathrm{min}} = -15$ eV with respect to the Fermi level). The denominator normalizes the PDOS weight below E_F, while the numerator yields the first moment of the occupied s-state distribution. To ensure consistent referencing of $\varepsilon_s^{\mathrm{bond}}$ across systems, this quantity is expressed relative to the $1s$ band center of an isolated H_2 molecule computed within the same simulation box:

$$\Delta\varepsilon_s^{\mathrm{bond}} = \varepsilon_{1s}^{\mathrm{bond}}(\mathrm{M{-}H}) - \varepsilon_{1s}^{\mathrm{bond}}(\mathrm{H{-}H}), \tag{5}$$

where $\varepsilon_{1s}^{\mathrm{bond}}(\mathrm{M{-}H})$ and $\varepsilon_{1s}^{\mathrm{bond}}(\mathrm{H{-}H})$ denote the bonding $1s$ levels associated with the surface-bound H atom and the H_2 molecule, respectively.

Similarly, the d-band center, ε_d, a widely used descriptor of metal reactivity and adsorp-

tion strength, is defined as

$$\varepsilon_d = \frac{\int_{E_{\min}}^{E_{\max}} E\, D_d(E)\, dE}{\int_{E_{\min}}^{E_{\max}} D_d(E)\, dE}, \tag{6}$$

where $D_d(E)$ is the d-projected density of states, and the integration range ($E_{\min}$ to $E_{\max}$) encompasses the full d-band manifold (typically -15 eV to $+5$ eV relative to E_F). However, no clear linear correlation between ε_d and the adsorption energies of either H or CO_2 is observed, suggesting that curvature introduces additional geometric and orbital effects beyond a simple electronic-structure descriptor.

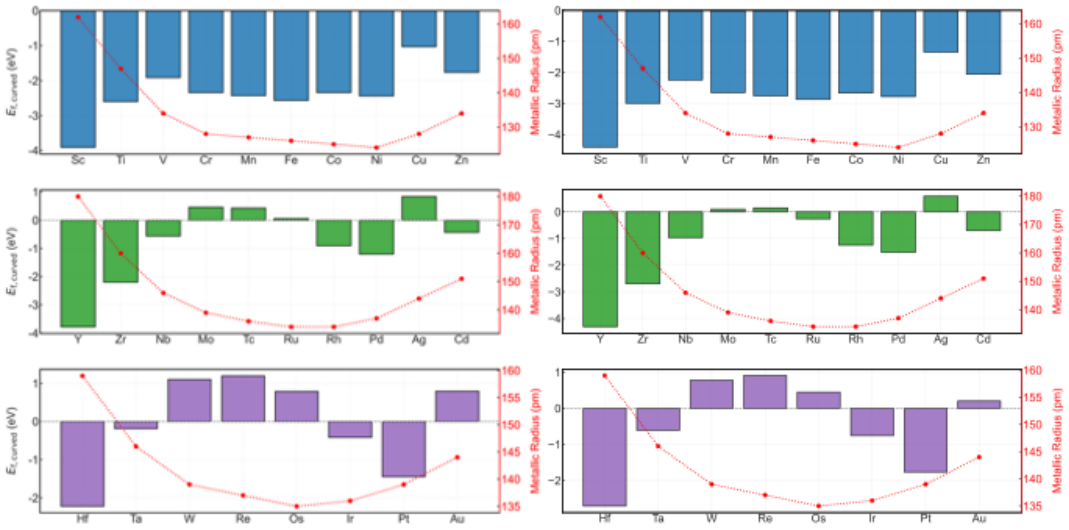

Figure S1: Comparison between formation energies (E_f) of curved surfaces at $\kappa = \pm 0.12$ Å^{-1} with and without the auxiliary hydrogen atom used to stabilize the curvature amplitude and width. Both cases exhibit consistent energetic trends across all metals, confirming that the added hydrogen introduces no chemical artifacts and that the qualitative curvature dependence remains unaffected.

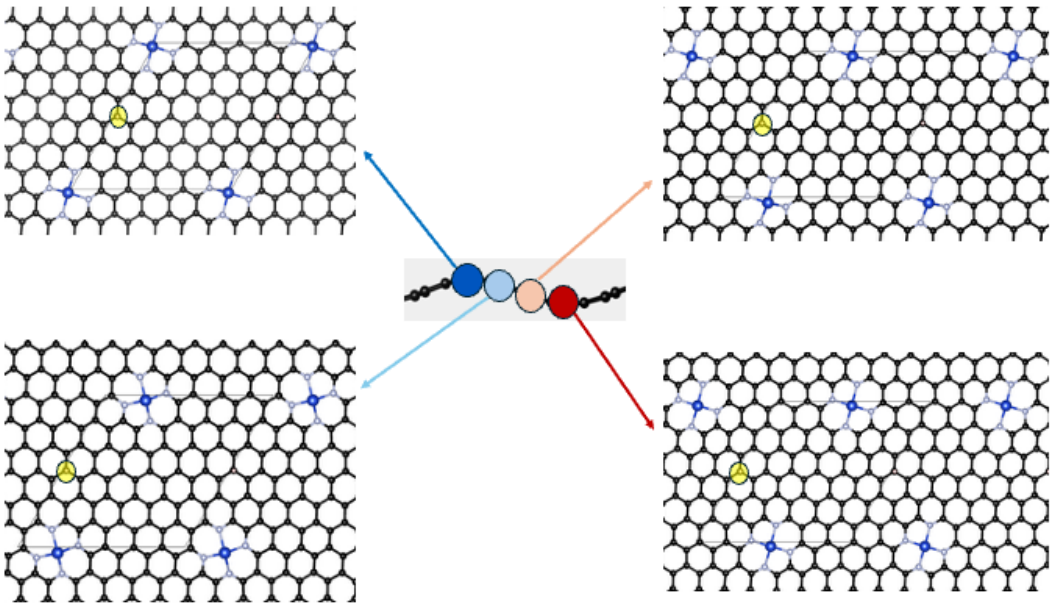

Figure S2: Geometry of the M–N_4 active sites showing the placement of the auxiliary hydrogen atom for the four curvature values studied.

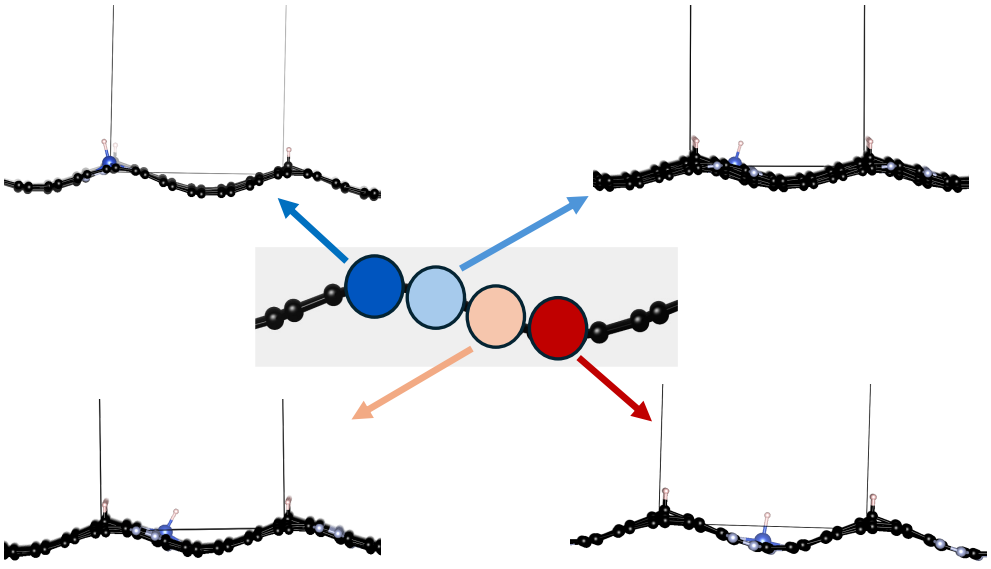

Figure S3: Optimized geometries of H-adsorbed M–N_4 sites (side view). The presence of the additional hydrogen atom preserves the curvature periodicity and structural pattern, enabling a consistent comparison of curvature effects on adsorption properties across metals.

2. Projected Density of States (PDOS) Analysis for H Adsorption

Figures S4–S6 illustrate curvature-dependent shifts in the metal d-band and hydrogen $1s$ states for M–N_4 single-atom catalysts upon hydrogen adsorption.

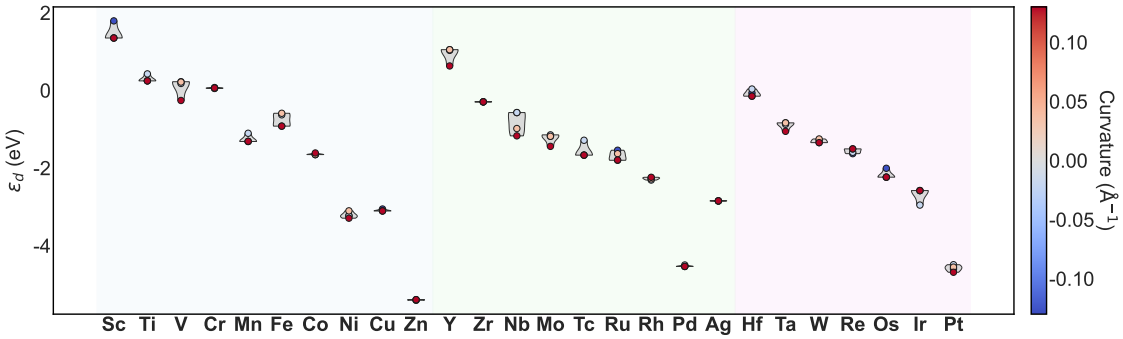

Figure S4: Violin plot showing the distribution of d-band centers (ε_d) relative to the Fermi energy of each specific system for M–N_4 sites (excluding Cd and Au) under H adsorption.

3. Projected Density of States (PDOS) Analysis for CO_2 Adsorption

Figures S7–S8 illustrate curvature-dependent shifts in the metal d-band for M–N_4 single-atom catalysts upon CO_2 adsorption.

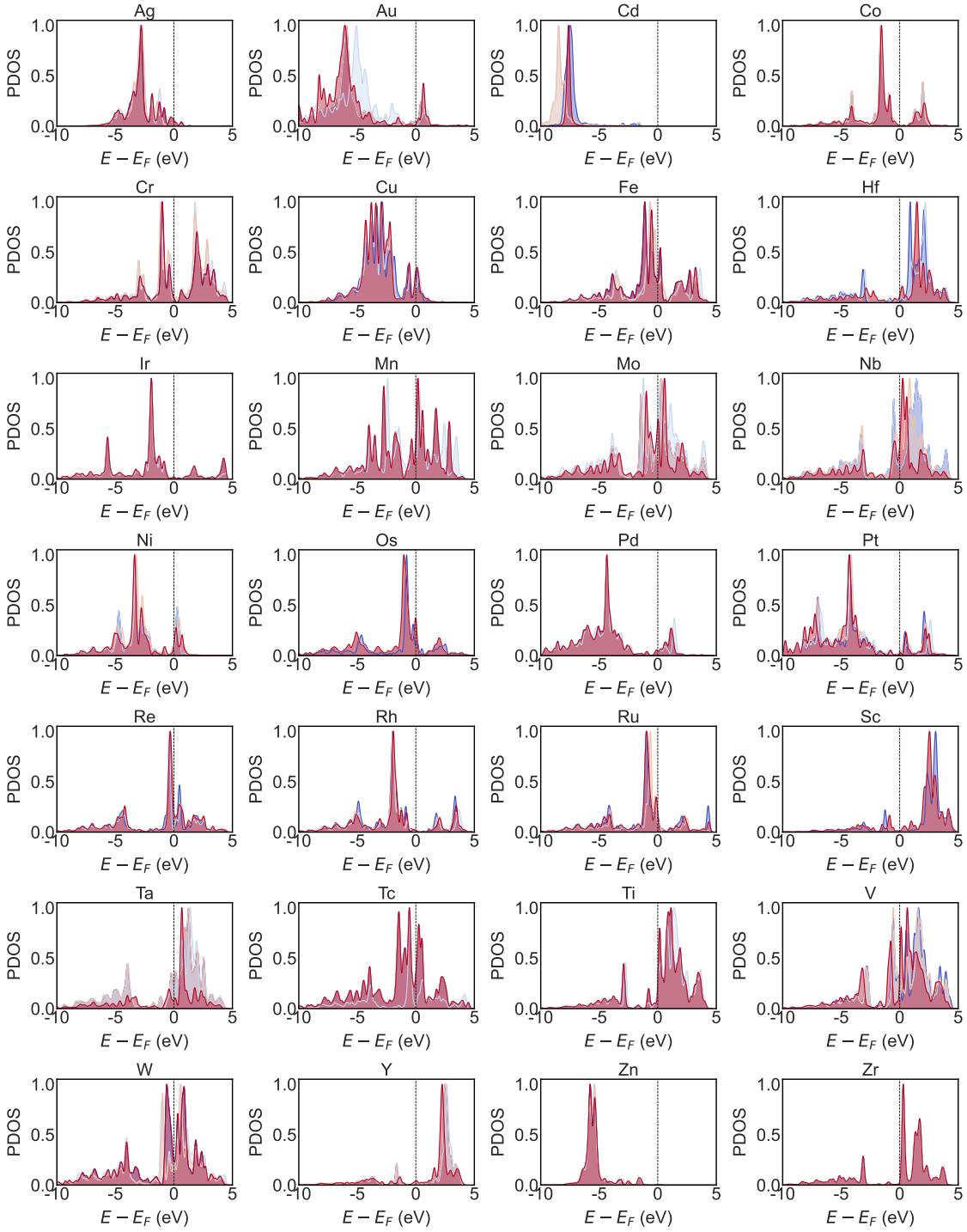

Figure S5: Curvature-resolved d-projected density of states (PDOS) of M in M–N_4 sites for H adsorption, plotted as a function of energy relative to the Fermi level ($E - E_F$). Each curve corresponds to a specific curvature, color-coded from blue (concave) to red (convex); color codes are consistent with Figure S4.

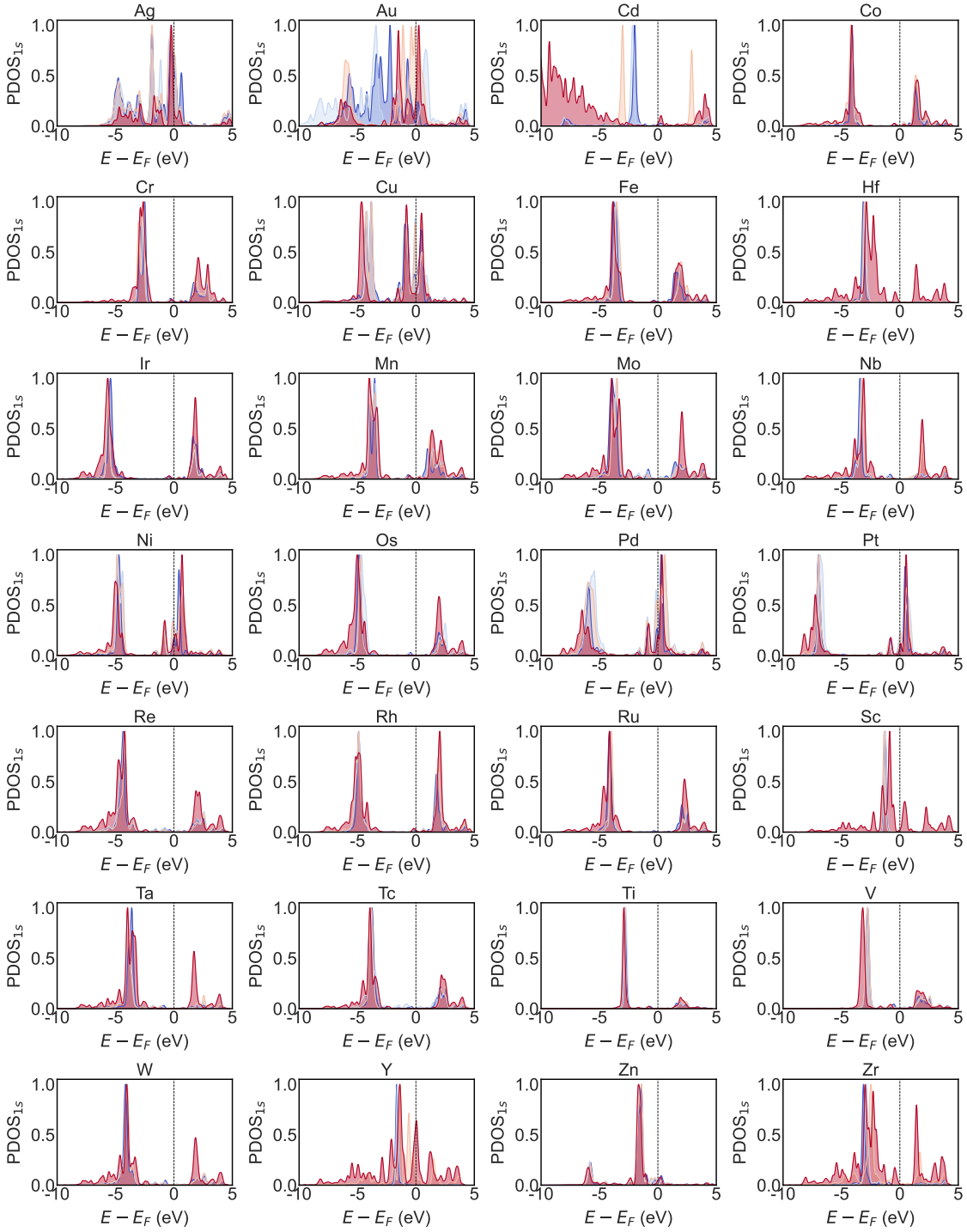

Figure S6: Curvature-resolved hydrogen 1s-projected density of states (PDOS) for all M–N_4–H systems. PDOSs are color-coded according to curvature (see Figure S7). The progressive upward shift of the 1s manifold under negative curvature indicates enhanced covalency in the M–H bond.

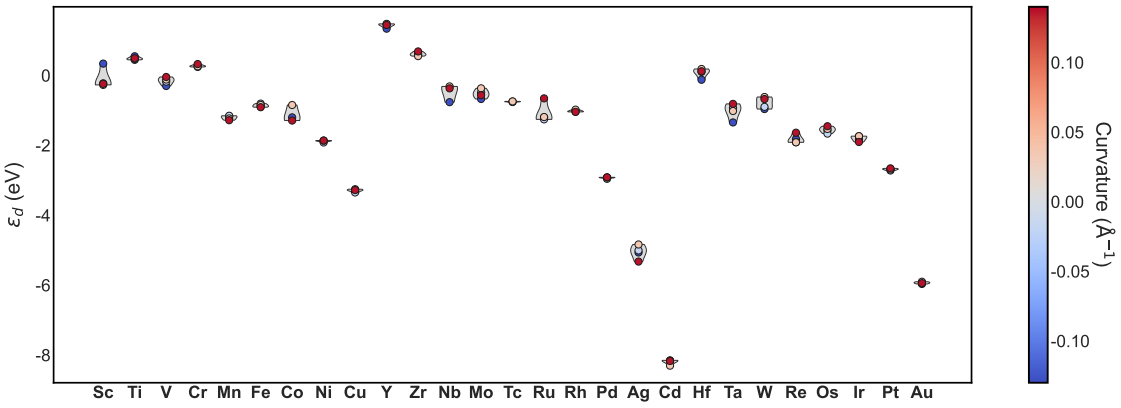

Figure S7: Violin plot showing the distribution of d-band centers (ε_d) relative to the Fermi energy of each specific system for M–N_4 sites (excluding Cd and Au) under CO_2 adsorption.

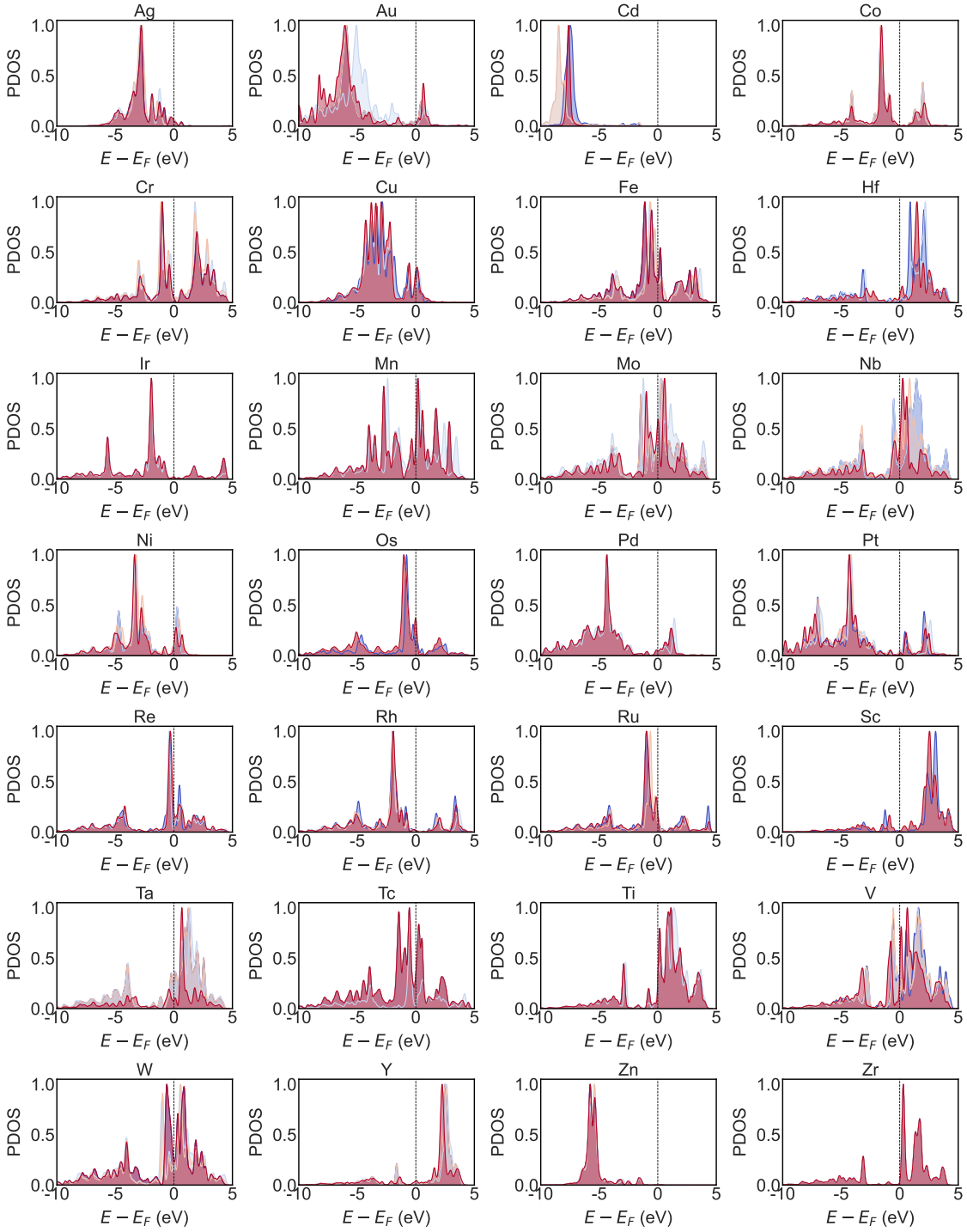

Figure S8: Curvature-resolved d-projected density of states (PDOS) of M in M–N_4 sites for CO_2 adsorption, plotted as a function of energy relative to the Fermi level ($E - E_F$). Each curve corresponds to a specific curvature, color-coded from blue (concave) to red (convex), consistent with Figure S7.

4. Steric Repulsion Analysis

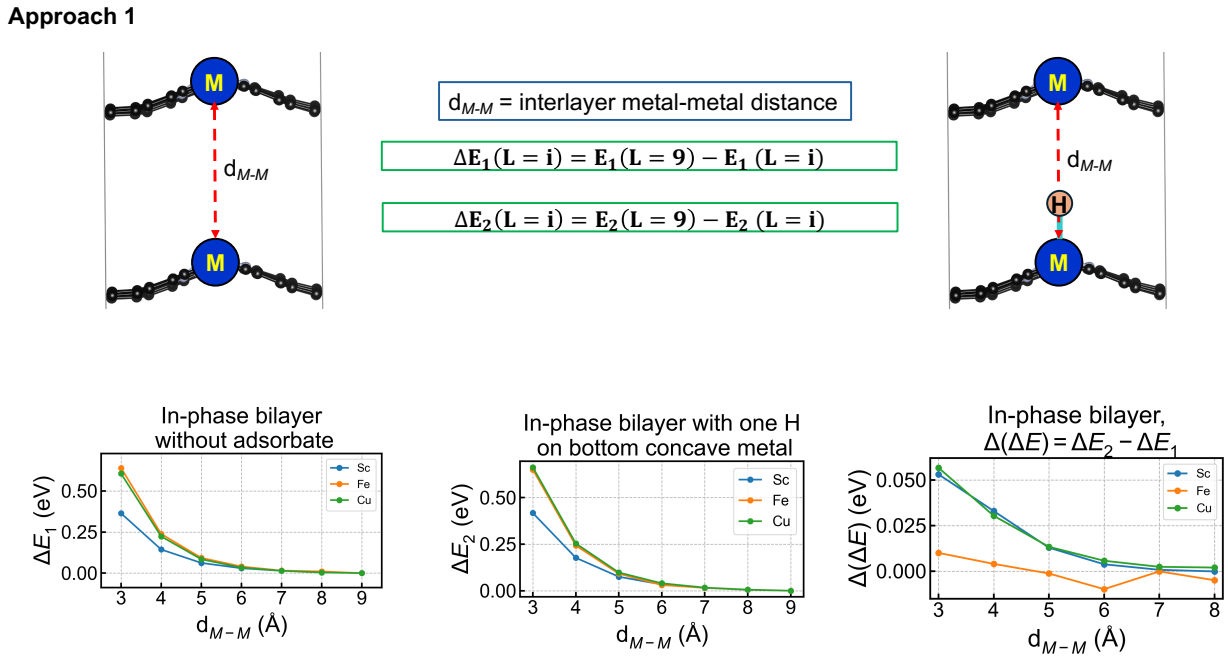

Figure S9: Quantification of steric interactions at the convex site upon H adsorption. Two concave layers are included to quantify the interaction, and $\Delta\Delta E$ denotes the net repulsion associated with the adsorbed H atom. For reference, the M–H bond distance is 1.5–1.9 Å.

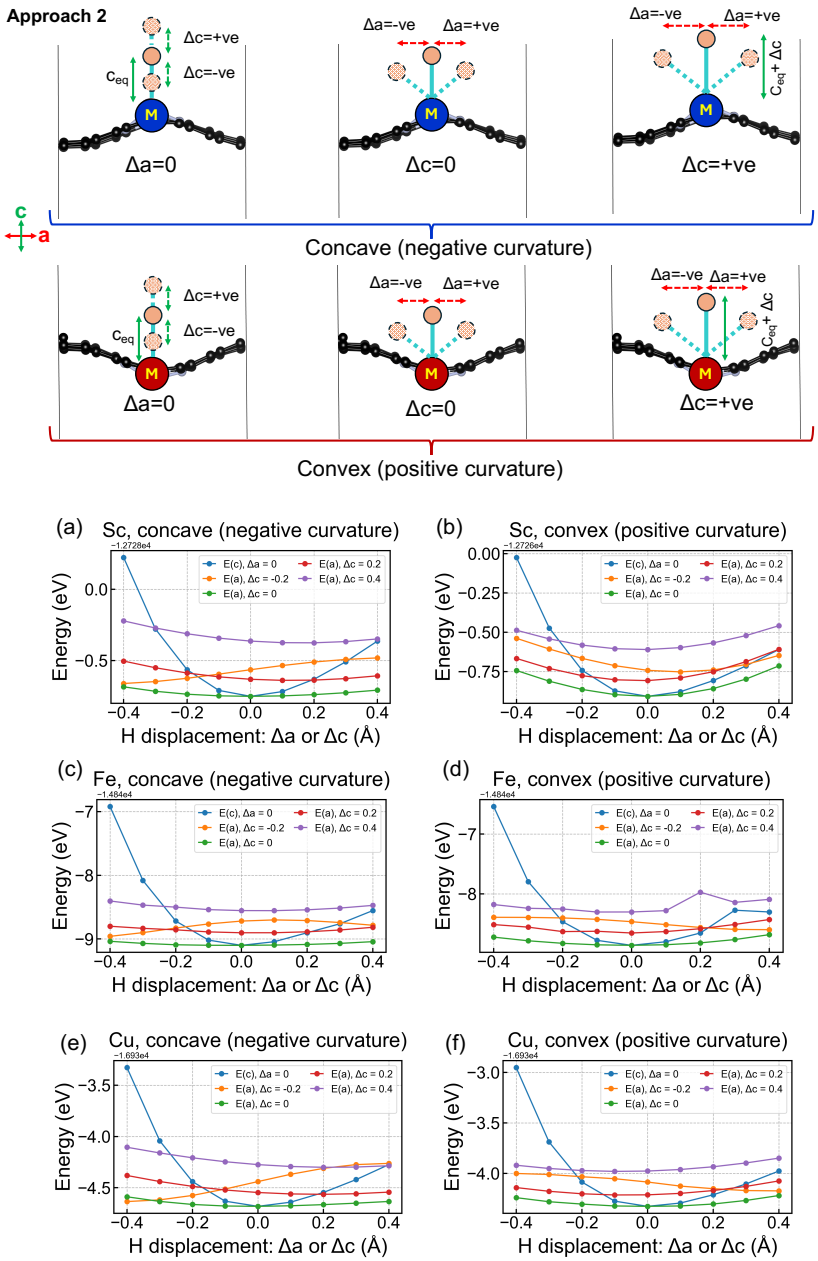

Figure S10: Potential energy surface (PES) plots for displacing the adsorbed H atom on the transition-metal (TM) site along the crystallographic a and c directions. Panels (a) and (b) correspond to TM = Sc with H adsorbed on the concave and convex faces, respectively. Panels (c) and (d) correspond to TM = Fe with H adsorbed on the concave and convex faces, respectively. Panels (e) and (f) correspond to TM = Cu with H adsorbed on the concave and convex faces, respectively. Here, Δa and Δc denote the displacements along the a and c directions, and $E(\Delta a)$ and $E(\Delta c)$ are the corresponding energy profiles. The notation $E(\Delta c)\,|_{\Delta a=n}$ denotes the energy as a function of displacement along c at a fixed displacement $\Delta a = n$.

References

(1) Giannozzi, P. et al. QUANTUM ESPRESSO: a modular and open-source software project for quantum simulations of materials. *Journal of Physics: Condensed Matter* **2009**, *21*, 395502.

(2) Perdew, J. P.; Burke, K.; Ernzerhof, M. Generalized Gradient Approximation Made Simple. *Physical Review Letters* **1996**, *77*, 3865–3868.

(3) Garrity, K. F.; Bennett, J. W.; Rabe, K. M.; Vanderbilt, D. Pseudopotentials for high-throughput DFT calculations. *Computational Materials Science* **2014**, *81*, 446–452.

(4) Grimme, S.; Antony, J.; Ehrlich, S.; Krieg, H. A consistent and accurateab initioparametrization of density functional dispersion correction (DFT-D) for the 94 elements H-Pu. *The Journal of Chemical Physics* **2010**, *132*.

(5) Monkhorst, H. J.; Pack, J. D. Special points for Brillouin-zone integrations. *Physical Review B* **1976**, *13*, 5188–5192.

(6) Banerjee, S.; Rappe, A. M. Mechanochemical Molecular Migration on Graphene. *Journal of the American Chemical Society* **2022**, *144*, 7181–7188.